Technical Note

Landslides
DOI 10.1007/s10346-025-02657-x
Received: 2 May 2025
Accepted: 6 November 2025

Rachele Franceschini · Nicola Nocentini · Ascanio Rosi · Lavinia Tunini · David Zuliani · Gabriele Peressi · Giuliana Rossi

Deriving rainfall thresholds with XAI and GNSS measurements for a large landslide

Abstract Landslides represent one of the most serious natural hazards in Italy, frequently resulting in fatalities and several damage to infrastructure. Recent advancements in Global Navigation Satellite Systems (GNSS) have enabled the development of monitoring systems that can monitor slope displacements continuously, accurately, and at relatively low cost. In this study, we present a monitoring network based on single-frequency GNSS sensors, integrated with rainfall data, applied to a large landslide affecting a village in the Carnic Alps (northern Italy). The objective is to showcase a practical example of continuous landslide monitoring using GNSS technology. By implementing a specific velocity threshold for GNSS measurements, we created an inventory of landslide reactivation events, which was then used to define rainfall thresholds based on data from two pluviometer stations. To enhance the interpretability of machine learning (ML) models used in the analysis, we adopted an innovative approach employing Partial Dependence Plots (PDPs). This technique allowed for a straightforward assessment of the influence of cumulative rainfall across various time windows, facilitating the identification of the most critical accumulation periods.

Keywords Landslides · GNSS · Rainfall · Monitoring systems

Introduction

Landslides are widespread in the Italian territory, and they cause the greatest number of losses of human lives and damages to infrastructures (Guzzetti 2000). In particular, slow-moving landslides (Hungr et al. 2014) can remain active for decades and can exhibit velocity variations in consequence to local environmental changes (Cascini et al. 2010) as precipitation. Determining the factors that control landslide occurrence is challenging because the relationship between landslides and the causative components varies spatially and temporally (Zhou et al. 2002). Nevertheless, a comprehensive understanding of these factors is important for the assessment of natural hazards (Borgomeo et al. 2014) and their direct impacts (Franceschini et al. 2022a). Landslide hazard can be reduced by adopting different mitigation methods: structural works and non-structural actions. If the former reduce the probability of occurrence of landslides, the latter, including Landslide Early Warning Systems (LEWS), are being increasing in recent years, mainly because of (i) their lower economic costs and environmental impact (Intrieri et al. 2012; Thiebes and Glade 2018); (ii) the development of new technologies for landslide monitoring (Crosta et al. 2017); (iii) the increasing availability of reliable databases to calibrate the warning models (Haque et al. 2016; Calvello and Pecoraro 2018). Furthermore, landslide EWSs collect valuable data that can be utilized for scientific research, monitoring, and landslide behavior analysis (Sapena et al. 2023).

One of the most used methodologies for early warning applications is rainfall thresholds, used to issue warnings when monitored rainfall exceeds a predefined level (Rosi et al. 2016; Segalini et al. 2018; Nocentini et al. 2024a, b). However, the landslide occurrence is not only related to rainfall intensity but also influenced by local conditions. Therefore, for an accurate early warning in large landslides, the measure of the local surface displacement is necessary.

Surface displacement's role in early warning systems for landslide detection has been a subject of research for a considerable period (Jaboyedoff et al. 2020; Fukuhara et al. 2023). The instruments commonly used for estimating landslide displacements are based on sensors installed in situ, such as inclinometers and extensometers, or remote sensing techniques using ground-based sensors, such as ground-based interferometric synthetic aperture radars (GBInSAR) (Pratesi et al. 2015; Carlà et al. 2019), terrestrial laser scanner, or topographic measurements captured by robotized total stations (Gigli et al. 2022; Beni et al. 2023; Innocenti et al. 2023). However, the complex and widespread nature of landslides necessitates accurate measurements, often with spatial coverage capable of targeting one or more slopes and an acquisition frequency high enough to catch substantial changes in the landslide (Casagli et al. 2023). Nowadays, remote-sensing techniques are becoming an indispensable tool in landslide investigation (Mantovani et al. 1996; Solari et al. 2020) and thanks to the development of modern monitoring technology such as global navigation satellite systems (GNSS), there have been substantial advances in Landslide Early Warning Systems (LEWSs). The advance in GNSS technology allowed for creating new sensors that can provide continuous monitoring with good precision and accuracy and limited costs (Benoit et al. 2015; Cina and Piras 2015; Zuliani et al. 2022a). For example, Notti et al. (2020) proposed a technical solution that adopts mass-market instrumentation, but also the definition of a monitoring systems management strategy that can be adapted to GNSS taking into consideration different phases: analysis, validation, interpretation and dissemination (bulletin) of obtained results. An automatic algorithm checks if the movements exceed statistical (related to instrument accuracy) and geological (defined according to geologic models and indicating potential critical phases) thresholds. If the movement exceeds the statistical threshold, an automatic alert report is generated with three alarm levels: green (normal conditions), yellow (first signal, waiting for a second measurement for confirmation), and red (alarm confirmed, requires geological validation), with manual control for alarm validation.

A successful LEWSs at the slope scale encompasses proper early warning indicators, primarily using monitored displacement and its velocity and, sometimes, environmental quantities, such as critical

water level and rainfall threshold (Berti et al. 2012; Intrieri et al. 2012; Huang et al. 2020; Wu et al. 2021). Rainfall thresholds, which define the rainfall levels beyond which landslides are likely to be triggered, are widely used in LEWSs due to their simplicity and rapid application. Traditionally, these thresholds are derived empirically by comparing a landslide inventory with rainfall intensity (I) and duration (D) data (Piciullo et al. 2018; Segoni et al. 2018a; Guzzetti et al. 2020). Although rainfall is indeed the primary trigger of landslides, using only these two parameters can overlook critical factors such as seasonal variations and antecedent soil moisture, both of which significantly increase the predisposition of a slope to landslide (Glade et al. 2000; Wicki et al. 2020). Only a limited number of studies have attempted to incorporate additional rainfall parameters alongside the traditional I-D threshold to enhance the cause-and-effect relationship between landslides and rainfall. Among them, Rosi et al. (2020) proposed a methodology to define three-dimensional (3D) rainfall threshold incorporating an additional axis to the I-D plane indicating the antecedent rainfall, to be used as a proxy for soil moisture condition.

More recently, artificial intelligence models have been used to attempt temporal landslide forecasting (Nava et al. 2023; Rosi et al. 2023; Mondini et al. 2023), but their use to derive rainfall thresholds is still unexplored.

While rainfall thresholds are generally designed for regional-scale forecasting (Krøgli et al. 2018; Jordanova et al. 2020; Zêzere et al. 2015), their use at the scale of individual landslides is far less common. Developing rainfall thresholds specifically for the reactivation of individual landslides is challenging, as active landslides may exhibit a different sensitivity to rainfall compared to new landslides (Intrieri et al. 2013; Bogaard et al. 2013; Vallet et al. 2016; Floris and Bozzano 2008). Ideally, thresholds should be calibrated separately for new and reactivated landslides to improve accuracy. However, landslide inventories rarely differentiate between new landslides and reactivations. Defining thresholds for reactivated landslides requires a robust monitoring system that provides a long-term record of reactivation events to ensure a reliable statistical analysis. Only a few studies have defined thresholds specifically for reactivated landslides. Wu et al. (2021) analyzed and defined a critical triggering threshold for LEWSs specifically for the Gapa landslide in south-western China. This landslide was reactivated by the water accumulation behind the first Jinping dam. Using GNSS data from last five years, a velocity threshold has been defined by an innovative method that uses a double moving average back and forward of time series. Since the deformation of the rockslide is closely related to changes in the water level of the reservoir, a critical water level has also been defined to reduce false alarms based only on the velocity threshold. Similar research has been conducted by Šegina et al. (2020). Authors analysed many GNSS stations, installed on a deep-seated landslide in Slovenia for establishing how different parts of the landslide react to precipitation.

In this work a monitoring network based on single-frequency GNSS sensors and its implementation for the definition of rainfall threshold for reactivations of a landslide involving a village in Italy is presented. The presence of the landslide affecting the town of Cazzaso (Municipality of Tolmezzo, Udine, Italy) in the north-eastern Alps was observed as early as the second half of the nineteenth century (CNR-GNDCI 1992). The landslide resulted in the displacement of the entire town by 24 m. For this reason, a new town was rebuilt in a new site 1 km away (Zuliani et al. 2022a). The work is based on the current monitoring system set up in agreement with the regional Civil Protection, that continuously records local displacement measures of the landslide body. The last report describes the triggering landslide (beginning of movement on one or more sensors equal to 1 cm/day) occurred with cumulative rains of duration equal to or greater than 3 days, with intensity equal to 42 mm/day and therefore a cumulative value of about 125 mm (Peressi 2019). Since the last report, new GNSS systems have been installed and this work aims to integrate and deepen the analyses and correlations between GNSS and rain. GNSS and rainfall thresholds and correlation between displacements and rainfall data are presented and discussed. The GNSS thresholds have been defined on the base of almost 9 years of observation (Zuliani et al. 2022a, b), while traditional I-D rainfall thresholds have been derived by MaCumBA software (Segoni et al. 2014a, b). This approach has been integrated with an innovative Machine Learning (ML) procedure to optimize the selection of the accumulation period that most influenced the reactivations of the Cazzaso landslide.

Study area

The village of Cazzaso (Municipality of Tolmezzo, Udine, Italy) lies at 680 m a.s.l., in the north-eastern sector of the Alpine mountain chain (Carnic Alps), and is located on a deep-seated landslide which is still active nowadays (Fig. 1a). The landslide affects a surface of approximately 2 km^2 with a sliding surface detected down to ~ 32 m below ground level through inclinometer measurements (Tunini et al. 2024a). Based on geomorphological reconstructions and geophysical surveys, the mobilized volume is estimated between 10^5 and 10^7 m^3 (Tunini et al. 2024a), hence falling within the large landslide class according to the classifications by Mc Coll & Cook (2024). The landslide body is constituted by glacial, fluvioglacial, lacustrine, and fluvial deposits (Colucci et al. 2014), lying on a calcareous–clayey bedrock (Fig. 1b). The superficial cover exhibits high lithological heterogeneity and variable permeability, which controls local drainage and preferential flow path (Zuliani et al. 2022a). The morphology of the slope is characteristic of post-glacial environment (Fig. 1c). It is classified by IFFI (Italian Inventory of Landslide. Trigila et al. 2007) as an earth rotational slide that has evolved into an earth flow. Historical data indicate reactivations since at least 1807, with a major event in October 1851, which caused a 24-m displacement of the original village, leading to the relocation of some buildings and the establishment of "Cazzaso Nuova" further downslope (CNR-GNDCI. 1992). Reactivations are associated with prolonged rainfall events, acting as primary triggering factors (Peressi 2019). Repeated topographic surveys and slope restoration interventions have been carried out in the area during the past and current decades (Coccolo 2010, 2012, 2015; Ramella and Roberto 2004, 2006). The landslide currently exhibits a slow rate of displacement on the order of meters per year, placing it within the "slow" category according to Cruden and Varnes (1996).

A characteristic longitudinal cross-section of the landslide is in Fig. 2. This section was developed by Tunini et al. (2024b), including borehole logs and inclinometer profiles. Topographic and lithological profiles used in the 2D limit equilibrium method (LEM) slope stability analysis are shown. Figure 2 illustrates two scenarios with differing groundwater conditions—one with a low-level and one with a high-level groundwater table in Profile 1—while in Profile 2 only a high-level groundwater scenario is considered. Both profiles present the most unstable sliding surface that corresponds to the

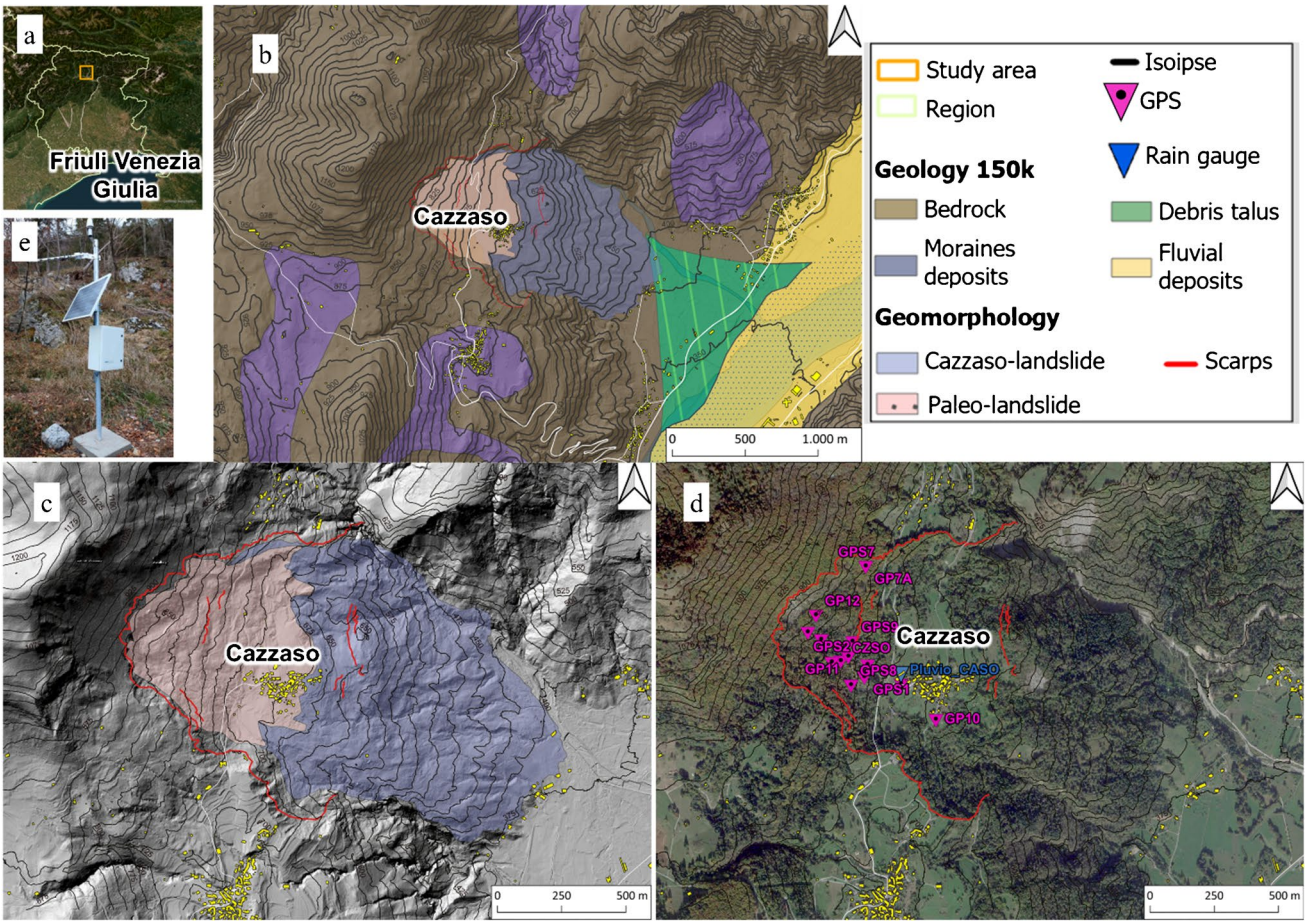

Fig. 1 In (**a**) localization of the area; (**b**) Geological setting of the study area; (**c**) Geomorphology of Cazzaso landslide. The hillshade has been used to basemap. The hillshade was derived from a 1 × 1 m digital terrain model (DTM). The DTM was derived from Friuli Venezia Giulia region web portal http://eaglefvg.regione.fvg.it; (**d**) Ortophoto and geolocalization of GNSS network. In (**e**) one of the GNSS stations on the Cazzaso landslide (in this case, GPS9)

easternmost part of the slope, delimited upstream by a morphological trench (Tunini et al. 2024a).

Current monitoring system

The Cazzaso landslide monitoring system has been deployed since 2016 by the Center for Seismological Research (CRS), belonging to the National Institute of Oceanography and Applied Geophysics—OGS. It is composed of 12 cost-effective single-frequency GPS stations (Fig. 1d and e) primarily located on the landslide body upslope the Cazzaso village, 1 geodetic-class dual-frequency GNSS station located in the Cazzaso village (CASO), 1 seismometric station equipped with an accelerometer and velocimeter and coupled with a single-frequency GNSS device (Zuliani et al. 2022b). The dual-frequency station CASO, equipped with a geodetic-level receiver (Trimble NetR9), tracks both L1 and L2 carrier signals from the GPS satellites, and it can provide position estimates with sub-millimetric level precision (Zuliani et al. 2022b; Tunini et al. 2024a). The monitoring system provides hourly displacement data for each geodetic site along the north, east, and vertical components, as well as displacements resulting from the average of the previous 24 h of observations. The displacements are calculated with respect to a reference station located out of the landslide body. The reference station is FUSE (or TOLS in the case of FUSE malfunctioning), belonging to the Friuli Regional Deformation Network-FReDNet, part of the north-eastern Italy monitoring system (SMINO) (Battaglia et al. 2003; Rossi et al. 2016, 2018; Zuliani et al. 2018; and Bragato et al. 2021; Tunini et al. 2024b) and located less than 3 km from the landslide. In this work, the reference configuration utilized to retrieve the displacements is "Net-Just" configuration, providing temporal continuity of the data. Based on the nature of the lithologies and similar case studies (Notti et al. 2020; Huang et al. 2022), three color-coded alert thresholds have been set for each of the GNSS stations, by the regional Civil Protection, considering a lapse of 24 h (Chersich et al. 2016; Bai et al. 2020, 2022; Zuliani et al. 2022a, b):

- In case the daily average movement rates exceed the limit of 1 cm, a yellow alert is issued. In relation to the data transmitted, in case of yellow alert (more than 1 cm/day) for GPS taken upstream of the city, an analysis of the evolutionary trend is implemented;
- If they exceed the limit of 2 cm, an orange alert is issued. If at least one GPS upstream of the village exceeds the threshold of

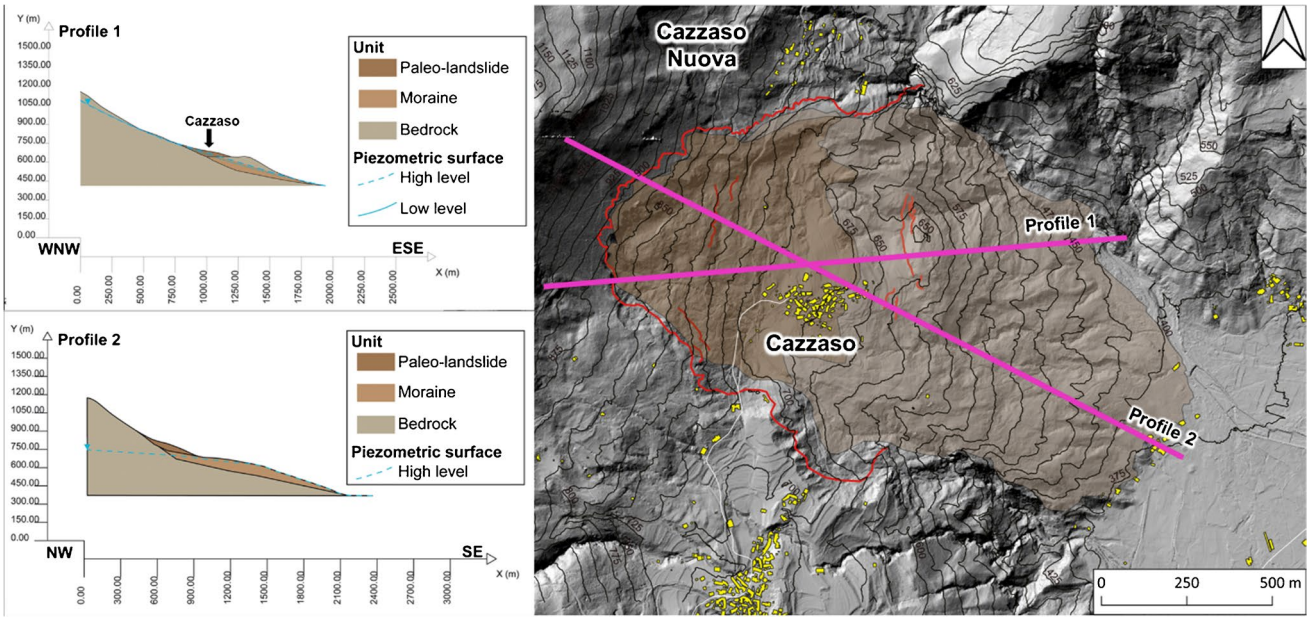

Fig. 2 Topographic and lithological profiles used for the 2D LEM slope stability analysis with two profiles in different conditions of water level. Profiles were derived by Tunini et al. 2024a

2 cm, the road Fusea-Cazzaso will be automatically interdicted to traffic.

- If they exceed at the limit of 3 cm, the alert will be red. If 3 GPS upstream of the village exceed the threshold of 3 cm/day, the village is evacuated.

In addition, if the region declares an orange weather alert for geological risk (rainfall capable of triggering landslide is expected), the closure of the Fusea-Cazzaso road is implemented as a preventive measure.

Materials

GNSS data

The time series of 12 GPS + 2 GNSS stations are analyzed. More than 540 thousand data, distributed from 2015 to 2024, have been examined. The system adopted for the configuration and control of the GPS network, as well for the data elaboration, called DISPLAYCE, is a cost-effective solution dedicated to monitoring of critical infrastructures and areas subject to slope instability (www.yettmoves.it/). DISPLAYCE software calculates the displacement of each station at regular intervals (i.e., regular sessions) of 1, 3, 6, 12, and/or 24 h, providing different parameters of the GPS signal (signal-to-noise ratio, number of cycle slips, etc.) (Tunini et al. 2024a, b). The calculation of the displacements is the result of the GPS data processing, which is carried out through the widely-known double difference (DD) technique (Kaplan et al. 1996; Hofmann-Wellenhof et al. 2001). Based on the current alert system, the first alarm threshold can be recorded by multiple GPS or GNSS stations and several times a day considering the horizontal or vertical component. To simplify data analysis, the module between the two components is calculated. For this work, the maximum speed (above the first threshold) recorded per day has been considered. This dataset represents an inventory of past reactivation events. In total, stations indicate a velocity above the first threshold 116 times (days) from 2016 to May 2024.

Rainfall data

CASO (Fig. 1d) and Tolmezzo stations are equipped with rain gauges which have been analyzed to obtain rainfall thresholds. The first pluviometer is located above landslide and the second station is located in Tolmezzo municipality almost 3.2 km from landslide. Both rain gauges provide hourly data, covering the period from 2016 to May 2024. CASO pluviometer is marked by more 56 thousand data, and it is part of the monitoring system managed by the Civil Protection. The data source about CASO pluviometer is DISPLAYCE software, which developed by yettmoves (www.yettmoves.it/). Tolmezzo pluviometer is characterized by more than 75 thousand data, and it is managed by ARPA FVG—SOC OSMER GRN—Osservatorio Meteorologico Regionale—Gestione Rischi Naturali Settore Meteo of CFD (Decentralized Functional Center—https://www.osmer.fvg.it/home.php) by Civil Protection of Friuli Venezia Giulia region.

The rainfall data has been analyzed to remove both low representative and noisy data: negative rainfall values or values higher than 200 mm/h and 0.2 mm/h have been removed, which are clearly erroneous (Nocentini et al. 2024a, b).

Methods

This chapter outlines the methods employed in order to provide a robust, data-driven framework that enhances the reliability and effectiveness of the generated LEWS:

1. At first, hourly deformation velocities have been calculated for each GNSS station. Daily velocity maxima over 1 cm/day have been then used to create an inventory of past reactivation events.
2. The cumulative rainfall from 1 to 30 days prior to each reactivation have been calculated. In this phase, reactivations not associate to rainfall have been removed from the analyses described below.
3. Intensity-duration rainfall thresholds have been defined using MaCumBA software.
4. Random Forest model and XAI (explainable AI) have been used to identify the most critical rainfalls.

I-D rainfall thresholds macumba

The threshold analysis was conducted using MaCumBA (Massive Cumulative Brisk Analyzer), a software firstly presented in Segoni et al. (2014a, b) and validated through numerous case studies in Italy (Rosi et al. 2015, 2021; Segoni et al. 2014a, b) and in other countries (Rosi et al. 2016, 2019). MaCumBA performs a semi-automated, rapid, and objective analysis, enabling the identification of rainfall thresholds based on the general power law initially proposed by Caine (1980):

$$I = \alpha D^{\beta}$$

where α and β are empirical parameters, proper of data distribution. One of the distinctive features of MaCumBA is the introduction of an additional parameter called No-Rain-Gap (NRG), which expresses the number of consecutive hours without rain needed to distinguish between rainfall events. This key parameter ensures replicability of the analysis and facilitates the implementation of thresholds in LEWS (Segoni et al. 2014a, b).

The software identifies the most representative I-D threshold encompassing 95% of landslide events. This threshold serves to distinguish the ordinary level, indicating no criticality, from the low criticality level. A successive calibration phase is performed to identify multiple thresholds, corresponding to higher landslide probabilities. The calibration of these higher thresholds is based on the number of acceptable False Alarms (FAs: alerts issued because rainfall exceeds the threshold, but no landslides occur), as introduced by Nocentini et al. (2024a). The moderate criticality threshold is determined by raising the low criticality threshold until a maximum of one FA per year is observed. The high criticality threshold is set by further raising the threshold until zero FAs are observed. This approach ensures a minimal number of FAs for the moderate and high criticality thresholds, making the system operationally efficient and more sustainable for the civil protection system (Nocentini et al. 2024a).

Random forest and variable importance for antecedent rainfall analysis

Traditional I-D thresholds consider only the rainfall event immediately preceding or coinciding with a landslide occurrence (Piciullo et al. 2018; Segoni et al. 2018b). However, this approach does not account for the effect of antecedent rainfall, which is particularly important for large landslides where the rainwater infiltrated into the soil need time to reach a deep slip surface (Glade et al 2000; Giannecchini et al. 2012; Kim et al. 2021; Rahul and Tyagi 2025). Therefore, relying only on I-D thresholds to evaluate the impact of rainfall on reactivating the Cazzaso landslide is insufficient. It is essential to also investigate how rainfall accumulated over extended periods affects these reactivations. However, there is no consensus in the literature on which accumulation period has the greatest influence on such triggers (Rosi et al. 2021; Salee et al. 2022; Nocentini et al. 2024a, b).

In order to determine the most relevant rainfall accumulation period affecting Cazzaso landslide reactivations, a ML approach has been evaluated. ML algorithms enable computers to learn from data, identifying logical patterns among them and making decisions based on that learned information (Hastie et al. 2001). These techniques are becoming popular worldwide because they allow to quickly process large datasets without requiring any statistical assumptions on their frequency distribution. The most sophisticated ML algorithms also provide interpretative metrics that allow verifying the reliability of model outcomes. As an example, in the field of landslide studies, these metrics can be assessed to evaluate if the logical reasoning learned by the model is plausible from a geomorphological perspective (Nocentini et al. 2023; Steger et al. 2024).

Specifically, we used the Random Forest (RF) algorithm (Breiman 2001; Catani et al. 2013), which offers several advantages, including the ability to calculate the Out-of-Bag Error (OOBE). This measure assesses the importance of each input variable by evaluating the potential error introduced when a specific variable is excluded (Molnar 2020). This model also allows the calculation Partial Dependence Plots (PDPs). The plots are a XAI technique that illustrates the marginal effect of a specific variable on the model's predictions, revealing the nature of the relationship (direct, inverse, or complex) between the input and landslide probability (Friedman 2001; Molnar 2020; Nocentini et al. 2024a, b; Schlögl et al. 2025).

The variables importance analysis (OOBE) was used to identify the most important accumulation period among different cumulative rainfall analysed; while PDPs were used to identify which rainfall value of the selected accumulation period had the greatest influence on landslide reactivations.

Several accumulation periods were considered to calculate cumulative rainfall: from 1 to 10 days with steps of 1 day, and periods of 15, 30, and 60 days. These values were calculated for all reactivation events above the 1 cm/day GNSS threshold (116 events, as described before). A non-reactivation dataset was also created by randomly sampling, within the study period, the same number of events, with velocities below the 1 cm/day threshold. This random sampling approach, widely supported in the literature (Catani et al. 2013; Reichenbach et al. 2018; Tehrani et al. 2022), helps prevent the unintentional selection of non-reactivation events associated with specific rainfall conditions, thereby ensuring a more representative and unbiased input for model training.

The database was then randomly divided into 80% training and 20% test datasets. The training set was used to train the model to identify a logical pattern between cumulative rainfall data and reactivations. By using the training set, the model also computes the variables importance and create the PDPs. The test set was used to evaluate the model's predictive capability. The model was implemented in MATLAB using the TreeBagger function for classification tasks. Apart from specifying the number of trees (500), all other

hyperparameters were left at their default settings, as they provided satisfactory performance during preliminary tests. By default, no limit is set on tree depth (trees grow until all leaves contain one observation, controlled by a MinLeafSize of 1); splits continue as long as a node has at least two observations; and the number of predictors considered at each split is set to the square root of the total number of input variables. The sensitivity analysis was performed by running the model 10 times, each run with a random division of training and test datasets, to assess its robustness to variations in input data. The variables importance was calculated for each run and then averaged. A random variable, with values between 0 and 1, was added as an additional input variable to test the model's ability to recognize its irrelevance and to verify the presence of overfitting issues. The RF model was trained with 500 trees, after its stability was verified with higher values during preliminary analysis. The model's accuracy was checked by the use of the Receiver Operating Characteristic (ROC) curve and the calculation of the AUC (Area Under the Curve, which ranges between 0 and 1) parameter, for both the rain gauges.

In order to clarify whether the reactivations of the Cazzaso landslide are primarily triggered by short and intense rainfall events or by antecedent rainfall, once the most important cumulative rainfall variable and its corresponding rainfall value with the highest influence were identified, a comparison with the performance of I–D thresholds is performed.

Results

GNSS and rainfall data

The comparison of the mean precipitation and the number of displacements above the velocity threshold is shown in Fig. 3, taking into account the comparison in temporal distribution on a monthly scale. On a monthly basis, the velocity threshold was exceeded mainly in fall and winter (October, November, December and January), while this was less frequent in summer from June to September (Fig. 3 black line). CASO and Tolmezzo rain gauges recorded an average annual rainfall of 1295.41 mm/year and 2081.2 mm/year, respectively. Regarding monthly rainfall averages, most rainy months were October and November for both rain gauges. January and August are characterized by less rain, with average rainfall values below 98.78 mm/month and 92.98 mm/month for CASO (Fig. 3 brown bars), while for Tolmezzo pluviometer, January and March are resulted to be months with less rainfalls, respectively with 107.88 mm and 136.40 mm (Fig. 3 yellow bars).

Rainfall thresholds macumba

The I-D thresholds for Cazzaso landslide were derived following the procedure outlined in "I-D Rainfall thresholds" section. Table 1

Table 1 I-D thresholds parameters for each pluviometer

Pluviometer	NRG (h)	α low criticality level (mm)	α moderate criticality level (mm)	α high criticality level (mm)	β (–)
CASO	30	7.3	18	72	–0.42
Tolmezzo	38	6.9	12	42	–0.41

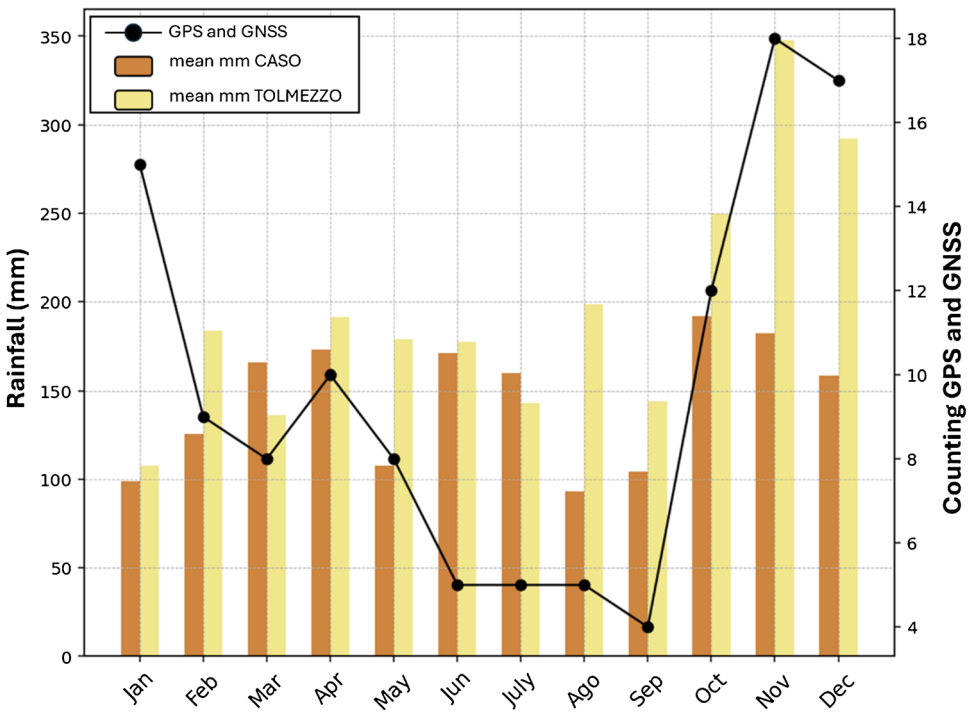

Fig. 3 Comparison on monthly base between mean rainfall and number of accelerations above the velocity threshold

summarizes the I-D threshold parameters for the three-criticality level obtained applying MaCumBA, while Table 2 shows their respective performance. A "No Rain Gap" (NRG) of 30 h with CASO and one of 38 h with Tolmezzo was derived from the ID thresholds (Table 1), respectively. An in-depth analysis of the thresholds (Table 2) revealed their low performances and reliability, since they were able to identify a correlation with only a few reactivations and issuing many false alarms. This result pointed out that the landslide reactivation may be linked to longer rain events, not detectable with I-D rainfall thresholds, or to different triggering factors.

Random forest and variables importance analysis

Once the RF model was trained and tested, its performances were verified. Considering the CASO rain gauge, average AUC of the test phase was 0.684 (± 0.055), while with Tolmezzo pluviometer data average AUC was 0.915 (± 0.046). This difference in results is linked with the higher completeness of rain time series of Tolmezzo station.

Even if the model trained with Tolmezzo data was more reliable than the one trained with CASO data, analysed described below were made considering both stations.

After RF model training and testing, XAI methods were applied to identify the most influent rainfall cumulation period and to derive rainfall thresholds. Figure 4 shows the importance estimates for each cumulative rainfall variable, calculated over the investigated accumulation periods (CR_x, where x represents the accumulation period in days) for CASO and Tolmezzo rain gauges. The bars represent the average importance obtained across 10 runs, while the whiskers indicate the observed range, from minimum to maximum values.

During preliminary analysis, the random variable showed a negative impact using both rain gauges, confirming that the model correctly identified it as irrelevant and even counterproductive in forecasting the reactivations. Therefore, the subsequent analyses were carried out without this variable. Since the random variable importance was negative, the hypothesis of overfitting could be discarded (Rosi et al. 2021, 2023). Using the CASO rain gauge, medium duration rainfalls, specifically 7, 8 and 9 days, exhibit the highest importance. While, for the Tolmezzo rain gauge, a strong importance of the 8-day cumulative rainfall emerges among others. In contrast, shorter accumulation periods (e.g., 1–3 days) and longer ones (e.g., over 30 days) show a lower influence on landslide activations for both rain gauges. These findings align with this type of landslide: the Cazzaso landslide is deep-seated, therefore short periods are insufficient to allow the infiltration and accumulation of enough water for the reactivation of the landslide. At the same time, the type of deposits (mainly glacial and fluvioglacial) where the landslide formed, means that rainy periods longer than a week are not necessary for the infiltrated rainwater to reach the sliding surface.

For the CASO rain gauge, the 7, 8, and 9-day cumulative rainfall values were selected for further analysis using PDPs, based on their high and similar importance. In contrast, for the Tolmezzo rain gauge, only the 8-day cumulative rainfall was selected, as it clearly has a higher OOBE value than other cumulation periods.

Partial dependence plots

PDPs have been used to visualize the effects of rainfalls on landslides reactivations, since they allow understanding the relationship between input variables (rainfall data in this case) and the trained learning models.

Figures 5 and Fig. 6 show the PDPs obtained for the CASO and Tolmezzo rain gauges, respectively, over ten model runs.

These plots display a consistent pattern across all cumulative rainfall durations analysed (7 in Fig. 5a, 8 in Fig. 5b, and 9 in Fig. 5c days for CASO; 8 days for Tolmezzo in Fig. 6): the predicted landslide probability initially increases with rainfall, reaches its maximum value, and then stabilizes, indicating a threshold beyond which additional rainfall does not further increase the reactivation probability. This behaviour aligns with the expected physical response: for each cumulation period, low rainfall values having limited influence, while higher cumulative rainfall contributes more on slope instability. This pattern is in line with actual knowledge of landslide behaviour and confirms the physical plausibility of the predictions.

For the CASO rain gauge, all three rainfall accumulation periods (CR_7, CR_8, and CR_9) showed a similar pattern, with peaks of importance at around 90 mm. These peaks were interpreted as critical rainfall thresholds beyond which the probability of landslide reactivation becomes significant. In contrast, for the Tolmezzo rain gauge, the most significant increase in importance was observed around 50 mm for the 8-day cumulative rainfall. This difference between the two rain gauges is likely due to the higher completeness of the Tolmezzo rainfall data, which may have enabled the

Table 2 I-D performance for each rain gauge. Correct Alarm (CA), MA Missed Alarm (MA) and False Alarm (FA)

	CASO			Tolmezzo		
	CA	MA	FA	CA	MA	FA
Low	11	15	54	2	7	73
Moderate	7	-	8	6	-	10
High	-	-	-	-	-	-
Total	18	15	62	8	7	83
Total reactivations detected	33			15		

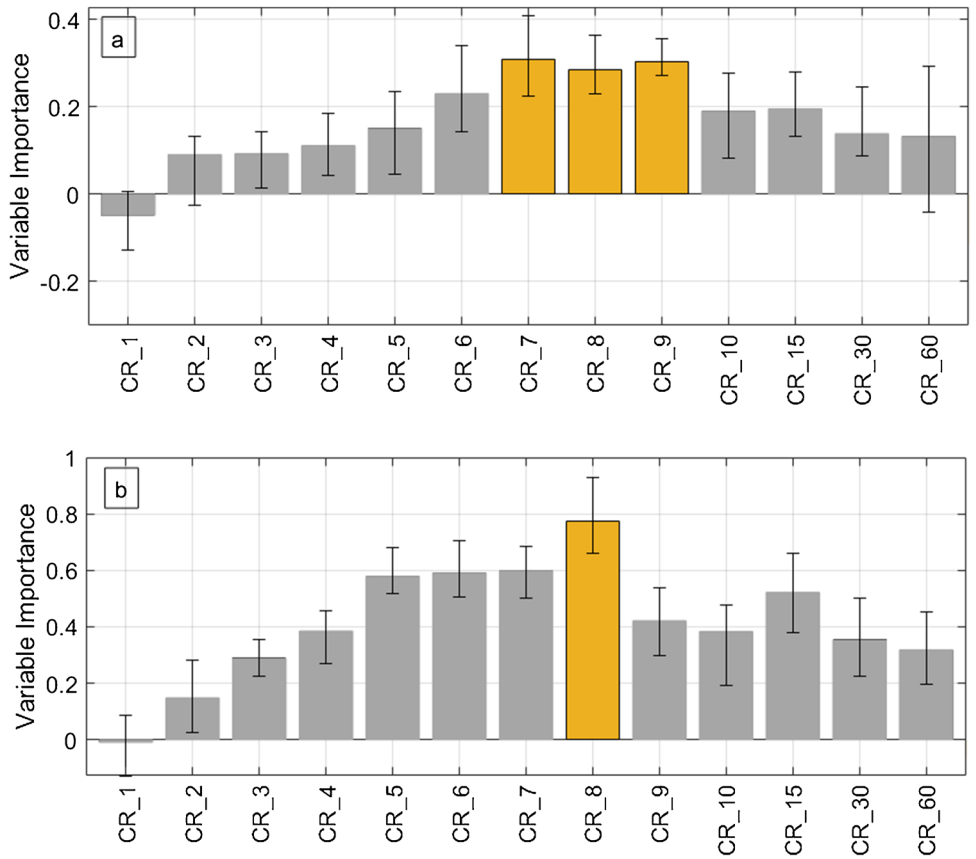

Fig. 4 Histogram of variable importance estimates for each cumulative rainfall variable tested, along with the random variable, for the rain gauges (a) CASO and (b) Tolmezzo

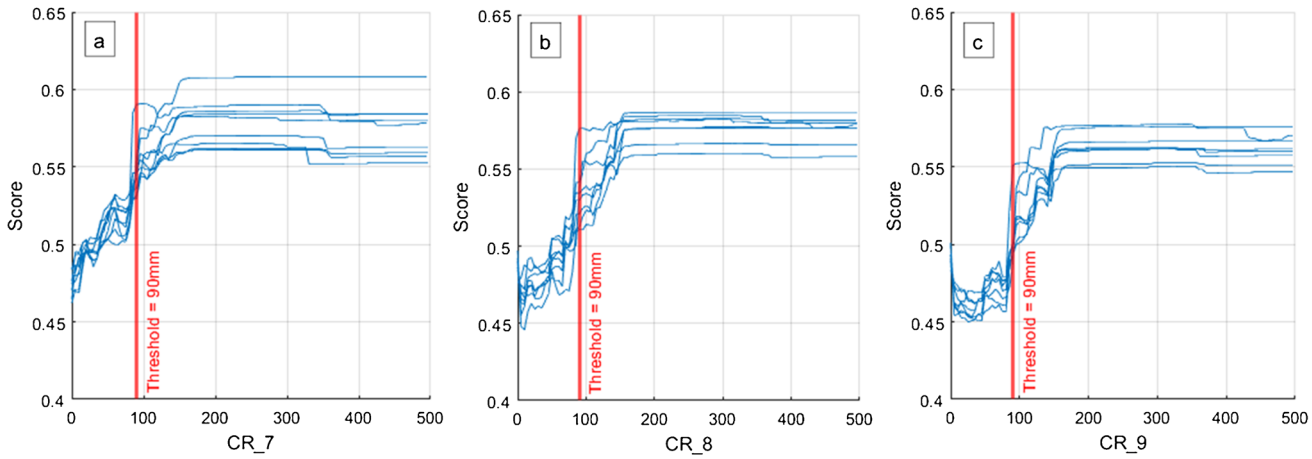

Fig. 5 PDPs obtained for different rainfall accumulation periods: (a) 7 days, (b) 8 days and (c) 9 days by using the CASO rain gauge. Red lines indicate rainfall thresholds and correspond to peaks in the gradient of variable importance

model to identify correlations between rainfall and landslide reactivations more accurately.

To assess the predictive capability of these thresholds and their applicability for a prototypal early warning system, a binary classification was performed to evaluate model performance in distinguishing reactivation vs. non-reactivation events for the whole observed period (2015-May 2024). Table 3 summarizes the performance metrics computed for each threshold.

For CASO, performance remains relatively stable across the three accumulation periods tested, with a slight increase in TP from CR_7 to CR_9. CR_9 led to the highest number of TP (47) but also resulted in the highest number of FP (286). On the other hand, the

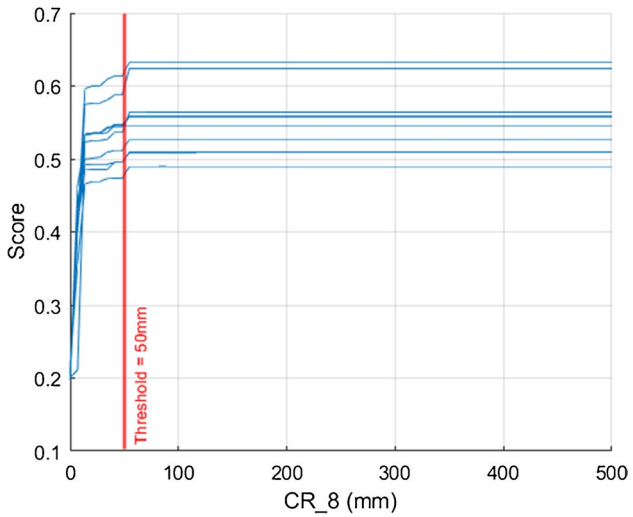

Fig. 6 PDPs obtained for the 8-day cumulative rainfall by using the Tolmezzo rain gauge. Red line indicates the rainfall threshold and corresponds to the peak in the gradient of variable importance

Table 3 Performance obtained using the rainfall thresholds identified with XAI

Rain gauge	Antecedent rainfall threshold	TP	FN	FP	TN
CASO	CR_7 = 90 mm	44	72	193	2657
	CR_8 = 90 mm	46	70	235	2615
	CR_9 = 90 mm	47	69	286	2564
Tolmezzo	CR_8 = 50 mm	72	44	992	2392

Tolmezzo threshold (CR_8 = 50 mm) achieved higher TP (72) but with a substantial increase in FP (992) due to the lower threshold.

From Table 3 also emerges the relatively low number of FN associated with Tolmezzo rain gauge (44) compared to higher values observed for the CASO thresholds (ranging from 69 to 72). This indicates that the Tolmezzo threshold is more effective at capturing reactivation events, even if at the cost of a higher number of FP. In operational EWSs contexts, minimizing FN is often prioritized, as missed alarms can result in severe consequences (Sättele et al. 2016; Guzzetti et al. 2020; Nocentini et al. 2024a, b). Therefore, the Tolmezzo threshold can be considered the most performant among those analysed for forecasting Cazzaso landslide reactivations. It is also worth noting that the 44 false negatives observed for the Tolmezzo threshold may not necessarily represent rainfall-induced reactivations. These could instead correspond to internal movements within the landslide body, such as slow creep, internal collapses, or compaction processes, which are not directly triggered by rainfall but are part of the landslide's natural kinematic evolution.

Finally, a comparison was made between rainfall thresholds and displacement thresholds derived from GNSS monitoring, as presented in Table 4. This comparison aimed to evaluate whether exceedances of antecedent rainfall thresholds correspond to significant ground displacements. When the CASO CR_9 threshold was exceeded, 20 GNSS measurements showed displacements over 3 cm/day, compared to 25 in the non-exceedance condition. This suggests that rainfall alone may not fully explain displacement patterns, and other triggering or preparatory factors might be involved. Similarly, for Tolmezzo, 25 displacements > 3 cm/day occurred during threshold exceedance, which is comparable to the 20 displacements observed when the threshold was not exceeded. These results highlight that while rainfall thresholds are effective in predicting reactivations, they may not always correspond to significant displacements, emphasizing the need for multi-sensor, multi-parameter early warning approaches.

Discussion

A landslide monitoring system is required to provide reliable and continuously updated data for quantitatively catching the scenario evolution, thus allowing a forecasting analysis and prompt actions for risk mitigation (Casagli et al. 2023). The monitoring of the spatial and temporal evolution of landslides is therefore crucial to evaluate the hazard, manage the risk, and define prevention and mitigation strategies (Cenni et al. 2021). The increasing availability of monitoring techniques, and thanks to the continuous improvement in data analysis techniques, research in the field of LEWS has seen remarkable advancements over the past decade. The identification of controlling factors of landslide occurrence is difficult, because the relationship between landslides and the causative components varies spatially and temporally (Zhou et al. 2002). Nevertheless, a full understanding of these factors is relevant for the assessment of natural hazards (Borgomeo et al. 2014) and of their direct effects (Franceschini et al. 2022a)

This study focuses on the deep-seated landslide affecting the area of Cazzaso (Tolmezzo, Udine), which extends over approximately 1.7 × 1.1 km. The geodetic monitoring system, operational since 2016 and developed by the Centro di Ricerche Sismologiche (CRS) of the Istituto Nazionale di Oceanografia e di Geofisica Sperimentale (OGS), in collaboration with the Regional Civil Protection, provides continuous displacement measurements, ensuring excellent temporal resolution of the data. The monitoring network

Table 4 Performance obtained by comparing the different GNSS thresholds levels with rainfall thresholds exceedance

	Antecedent Rainfall Threshold			
	CASO		Tolmezzo	
GNSS threshold	CR_9>90mm	CR_9<90mm	CR_8>50mm	CR_8<50mm
>1cm & <2cm	19	34	36	17
>2cm & <3cm	8	10	11	7
>3cm	20	25	25	20

currently covers a limited area of approximately 200 × 250 m, primarily concentrated around the inhabited zone. This spatial constraint is a result of strategic choices aimed at civil protection, prioritizing potentially hazardous surface movements near the village. The monitoring system comprises 12 single-frequency GPS stations and 2 dual-frequency GNSS stations, complemented by one rain gauges, allowing for integrated analysis of displacement time series and precipitation data. While the network is not designed to detect large landslide deformations, it provides reliable and continuous measurements of superficial slope movements within and immediately upslope of the village (Tunini et al. 2024b; Zuliani et al. 2022a). In addition to GNSS monitoring, multi-temporal InSAR and LiDAR analyses have been employed to enhance the understanding of the landslide's kinematics and morphology. These datasets have been integrated into 2D and 3D numerical stability models, contributing to hazard assessment and early warning efforts for this deep-seated moraine-based landslide system (Tunini et al. 2024a; Buono et al. 2025). Landslide activity in this area has been historically documented since at least 1807. A significant event occurred in October 1851, when a rotational–flow movement destroyed a portion of the original settlement, prompting the foundation of 'Cazzaso Nuova' approximately 1 km downslope. More recent observations also indicate superficial mass movements involving the upper slope and the inhabited sector. For example, 5/03/2016; 3/04/2024 and 15/05/2024, Friuli Venezia Giulia Civil Protection notices significant events of the landslide due to heavy rainfall of the past few days. Some phenomena were also surveyed within the multi-risk information gateway landslide inventory from newspaper reports (developed by Battistini et al. 2013) and classified by Franceschini et al. (2022b) From this inventory, it is possible to extract additional reactivations in the years affecting the area: 29/04/2017; 06/12/2020; 02/11/2023; 03/04/2024; involving also a road closure due to landslide movement.

In previous works (Peressi 2019), the landslide was identified as rainfall-driven, so the definition of statistical rainfall threshold was initially attempted, for establishing warning levels. This approach led to the definition of I-D thresholds; however, their validation revealed poor performances and unreliability. Given that the Cazzaso landslide is quite large and deep, it is possible that simple empirical/statistical approaches are inadequate to depict its complex internal rheology, hence more sophisticated models should be used. For defining rainfall thresholds, two stations have been analysed. Even if CASO rain gauge could be considered highly representative as it is located inside the sliding mass, time series were incomplete, with several data interruption, so data from Tolmezzo rain station were used as well. Although the Tolmezzo rain gauge provides a longer and more continuous record, its greater distance from the landslide may make rainfall measurements slightly less representative of local conditions. For a more effective early-warning implementation, it would therefore be important to improve the continuity and reliability of the CASO rain gauge, and to repeat the analyses once a longer and complete dataset becomes available, in order to refine and validate the rainfall thresholds. It is important to note that the GNSS network supports a monitoring objective rather than a real-time early warning function. As such, the data are analyzed over daily timescales to detect trends in surface displacement, rather than to activate immediate response protocols. The monthly distribution of GNSS data and precipitation showed a seasonal trend. In the fall and winter months (from October to March), the number of GNSS threshold exceedances increases, while the amount of precipitation usually remains relatively constant.

An approach based on RF model and XAI techniques (OOBE to define variables importance and PDPs to visualize their influence) was used to identify the most influential rainfall parameters. The results highlighted that medium-term cumulative rainfall (7, 8, and 9 days considering CASO rain station and 8 days considering Tolmezzo pluviometer), has the greatest impact on landslide reactivation.

For the Tolmezzo rain gauge, the rainfall threshold of 50 mm over 8 days resulted in the lowest number of FN, demonstrating higher predictive performance compared to the thresholds identified with RF for the CASO rain gauge and the traditional I–D method (only 15 reactivation events were correctly associated with rainfall using I–D thresholds for Tolmezzo). The inconsistency in results of ID thresholds and the relatively high number of FN in the RF models, combined with the well-known seismicity of the area, suggested the possibility of the coexistence of different triggering factors. To investigate this hypothesis, the database provided by CRS (https://terremoti.ogs.it/) was used to identify earthquakes with a magnitude greater than 2. It includes earthquakes that occurred in north-eastern Italy and the surrounding area from January 1, 1977, to the present day. However, no correlation between reactivations and seismic events was identified. Data from accelerometer and velocimeter located in CASO station (in Cazzaso village) were analysed as well, considering 3 days before and after each landslide reactivation. No signals attributable to the landslide movement were detected. These findings of this work are consistent with the geomorphological characteristics of the landslide. While short rainfall events are insufficient to induce reactivation due to limited infiltration amount of water that can infiltrate, very long accumulation periods may not be necessary, as the failure surface is not extremely deep and the soil can be considered as medium permeability. The histograms of variables importance (Fig. 2) also revealed that daily rainfall has minimal or even negative importance for the model's predictive performance. These findings align with actual understanding of the response to rainfall of deep landslides. However, due to a lack data, the current work does not account for subsurface hydrological states (e.g., soil moisture, groundwater), which can strongly modulate the slope response to rainfall. Future work should integrate such variables to improve the knowledge of landslide behavior, leading to the definition of a refine landslide model, which is essential to properly set-up a proper LEWS.

Overall, these results confirm the robustness of the proposed ML framework in identifying rainfall thresholds that are both physically meaningful and operationally effective. This approach provides an innovative way to identify reliable rainfall thresholds. Nevertheless, rainfall thresholds should be re-estimated in view of changes in rainfall intensity and duration. Indeed, landslide risks could be exacerbated by global changes such as increased in the frequency or magnitude of rainfall (Patton et al. 2019). The empirical thresholds used in the current system are based on historical rainfall–displacement relationships, which may evolve due to climate variability. Future developments could include the integration of non-stationary models or probabilistic approaches to

dynamically update threshold values, enhancing the system's long-term robustness.

Conclusions

The work is based on the current monitoring system adopted and in place by CRS – National Institute of Oceanography and Applied Geophysics—OGS. The aim of this work is to extract rainfall thresholds for landslide reactivations. The monitoring system each hour automatically acquires data from GPS/GNSSs and rain gauge. By applying a velocity threshold specifically for GPS/GNSS instruments, it was possible to create an inventory of landslide reactivations, a novel aspect that provides valuable insights for conducting important analyses. Since traditional empirical approaches failed to define reliable rainfall thresholds for the case of study an innovative approach based on the interpretability of ML algorithms was used to identify rainfall thresholds. The use of PDPs allowed for a rapid and simple evaluation of the influence of cumulative rainfall over multiple time windows, enabling the identification of the most significant accumulation period in a straightforward way. This framework proved to be particularly effective in a context where traditional I–D threshold methods failed to capture the triggering conditions of the Cazzaso landslide, since the landslide is not directly influenced by short-duration and intense rainfall. In contrast to I–D approaches, the ML-based analysis successfully revealed that the 8-day cumulative rainfall is the most relevant predictor of reactivation, providing reliable thresholds for supporting GNSS system for operational warning purposes. The proposed methodology can be applied to assess the role of short and long terms rainfalls in landslide reactivations across different geomorphological and climatic settings, as it based on rainfall and displacement data. However, rainfall thresholds should be re-estimated when a consistent number of new GPS/GNSS acquisition will be available, in view of changes in rainfall intensity and duration, due to climate changes. While tailored to a specific site, the detailed outline of this tool can be valuable in addressing similar situations. Furthermore, some of these solutions may be broadly applicable, even in entirely different contexts.

Acknowledgements

The authors wish to thank the Civil Protection of the Friuli Venezia Giulia Region, for the collaboration in the realization of the early warning system described in this paper and for the precious work in collaboration with Center for Seismological Research (CRS—National Institute of Oceanography and Applied Geophysics – OGS) for the monitoring system.

Author contribution

Text writing: R.F., N.N., A.R. Data analysis: R.F. and N.N. Conceptualization: L.T, R.F., D.Z. and G.P. Manuscript reviewing: L.T. and A.R. Supervisor: D.Z and G.R.

Funding

This study was carried out within the RETURN Extended Partnership and received funding from the European Union Next-GenerationEU (National Recovery and Resilience Plan – NRRP, Mission 4, Component 2, Investment 1.3 – D.D. 1243 2/8/2022, PE0000005).

Declarations

Competing interests The authors did not receive support from any organization for the submitted work.

References

Bai D, Tang J, Lu G, Zhu Z, Liu T, Fang J (2020) The design and application of landslide monitoring and early warning system based on microservice architecture. Geomat Nat Hazards Risk 11(1):928–948. https://doi.org/10.1080/19475705.2020.1766580

Bai D, Lu G, Zhu Z, Zhu X, Tao C, Fang J (2022) A hybrid early warning method for the landslide acceleration process based on automated monitoring data. Appl Sci 12(13):6478. https://doi.org/10.3390/app12136478

Battaglia M, Zuliani D, Pascutti D, Michelini A, Marson I, Murray MH, Bürgmann R (2003) Network assesses earthquake potential in Italy's southern Alps. Eos Trans Am Geophys Union 84(28):262–264. https://doi.org/10.1029/2003EO280003

Battistini A, Segoni S, Manzo G, Catani F, Casagli N (2013) Web data mining for automatic inventory of geohazards at national scale. Appl Geogr 43:147–158

Beni T, Boldini D, Crosta GB, Frodella W, Gallego JI, Lusini E, Spizzichino D (2023) Rock instabilities at the archaeological site of Dadan (Kingdom of Saudi Arabia). Landslides 20(11):2455–2478. https://doi.org/10.1007/s10346-023-02122-7

Benoit L, Briole P, Martin O, Thom C, Malet JP, Ulrich P (2015) Monitoring landslide displacements with the Geocube wireless network of low-cost GPS. Eng Geol 195:111–121. https://doi.org/10.1016/j.enggeo.2015.05.020

Berti M, Martina MLV, Franceschini S, Pignone S, Simoni A, Pizziolo M (2012) Probabilistic rainfall thresholds for landslide occurrence using a Bayesian approach. J Geophys Res Earth Surf. https://doi.org/10.1029/2012JF002367

Bogaard T, Maharjan LD, Maquaire O, Lissak C, & Malet JP (2013). Identification of hydro-meteorological triggers for Villerville coastal landslide. In: Margottini, C., Canuti, P., Sassa, K. (eds) Landslide Science and Practice. Springer, Berlin, Heidelberg. https://doi.org/10.1007/978-3-642-31427-8_18

Borgomeo E, Hebditch KV, Whittaker AC, Lonergan L (2014) Characterising the spatial distribution, frequency and geomorphic controls on landslide occurrence, Molise, Italy. Geomorphology 226:148–161

Bragato PL, Comelli P, Saraò A, Zuliani D, Moratto L, Poggi V, Parolai S (2021) The OGS–Northeastern Italy seismic and deformation network: current status and outlook. Seismol Res Lett 92(3):1704–1716. https://doi.org/10.1785/0220200372

Breiman L (2001) Random forests. Mach Learn 45:5–32. https://doi.org/10.1023/A:1010933404324

Buono G, Nutricato R, Facchi P, Guerriero L, Pepe FV, Lupo C, & Pascazio S (2025). Compared analysis of DInSAR data from ascending and

descending orbits of Sentinel-1: the Cazzaso case study. arXiv preprint arXiv:2504.12306.
Caine N (1980) The rainfall intensity: duration control of shallow landslides and debris flows. Geogr Ann Ser A Phys Geogr. https://doi.org/10.1080/04353676.1980.11879996
Calvello M, Pecoraro G (2018) Franeitalia: a catalog of recent Italian landslides. Geoenviron Disasters 5:13. https://doi.org/10.1186/s40677-018-0105-5
Carlà T, Tofani V, Lombardi L, Raspini F, Bianchini S, Bertolo D, Casagli N (2019) Combination of GNSS, satellite InSAR, and GBInSAR remote sensing monitoring to improve the understanding of a large landslide in high alpine environment. Geomorphology 335:62–75. https://doi.org/10.1016/j.geomorph.2019.03.014
Casagli N, Intrieri E, Tofani V, Gigli G, Raspini F (2023) Landslide detection, monitoring and prediction with remote-sensing techniques. Nat Rev Earth Environ 4(1):51–64. https://doi.org/10.1038/s43017-022-00373-x
Cascini L, Cuomo S, Pastor M, Sorbino G (2010) Modeling of rainfall-induced shallow landslides of the flow-type. J Geotech Geoenviron Eng 136(1):85–98
Catani F, Lagomarsino D, Segoni S, Tofani V (2013) Landslide susceptibility estimation by random forests technique: sensitivity and scaling issues. Nat Hazards Earth Syst Sci 13:2815–2831. https://doi.org/10.5194/nhess-13-2815-2013
Cenni N, Fiaschi S, Fabris M (2021) Integrated use of archival aerial photogrammetry, GNSS, and InSAR data for the monitoring of the Patigno landslide (Northern Apennines, Italy). Landslides 18(6):2247–2263. https://doi.org/10.1007/s10346-021-01635-3
Cina A, Piras M (2015) Performance of low-cost GNSS receiver for landslides monitoring: test and results. Geomat Nat Hazards Risk 6(5–7):497–514. https://doi.org/10.1080/19475705.2014.889046
CNR-GNDCI. Consiglio Nazionale delle Ricerche, Gruppo Nazionale per la Difesa dalle Catastrofi Idrogeologiche. Progetto AVI (Aree Vulnerate Italiane)—Archivio Frane. Scheda di Censimento n. 1300218. 1992. Available online: http://wwwdb.gndci.cnr.it/php2/avi/frane_tutto.php?numero_frana=1300218&lingua=it (accessed on 28 April 2022).
Coccolo A. Realizzazione di una rete di Monitoraggio con Metodologia GPS Nell'ambito Dell'intervento Relativo al Monitoraggio del Movimento Franoso a Monte di Cazzaso. Rete di Monitoraggio GPS14, Monografie dei Caposaldi, MON; Technical report realised by CP Ingegneria consulting engineers for the Tolmezzo Municipality; Municipality: Tolmezzo, Italy, 2010.
Coccolo A. Realizzazione di una Rete di Monitoraggio con Metodologia GPS Nell'ambito Dell'intervento Relativo al Monitoraggio del Movimento Franoso a Monte di Cazzaso. Rete di Monitoraggio GPS14, Relazione Illustrativa, REL; Technical report realised by CP Ingegneria consulting engineers for the Tolmezzo Municipality; Municipality: Tolmezzo, Italy, 2012.
Coccolo A. Realizzazione di una Rete di Monitoraggio con Metodologia GPS Nell'ambito Dell'intervento Relativo al Monitoraggio del Movimento Franoso a Monte di Cazzaso. Rete di Monitoraggio GPS14, Campagna di Misure n°16, 9–10 Dicembre 2015, R16; Technical report realised by CP Ingegneria consulting engineers for the Tolmezzo Municipality; Municipality: Tolmezzo, Italy, 2015.
Colucci RR, Monegato G, Žebre M (2014) Glacial and proglacial deposits of the Resia Valley (NE Italy): new insights on the onset and decay of the last Alpine Glacial Maximum in the Julian Alps. Alp Mediterr Quat 27(2):85–104
Crosta GB, Agliardi F, Rivolta C, Alberti S, Dei Cas L (2017) Long-term evolution and early warning strategies for complex rockslides by real-time monitoring. Landslides 4(5):1615–1632. https://doi.org/10.1007/s10346-017-0817-8
Cruden DM, & Varnes DJ (1996). Landslide types and processes. In: Turner AK, Schuster RL (eds) Landslides investigation and mitigation. Transportation research board, US National Research Council. Special Report 247, Washington, DC, Chapter 3, pp. 36–75
Floris M, Bozzano F (2008) Evaluation of landslide reactivation: a modified rainfall threshold model based on historical records of rainfall and landslides. Geomorphology 94(1):40–57. https://doi.org/10.1016/j.geomorph.2007.04.009
Franceschini R, Rosi A, Del Soldato M, Catani F, Casagli N (2022a) Integrating multiple information sources for landslide hazard assessment: the case of Italy. Sci Rep 12(1):20724. https://doi.org/10.1038/s41598-022-23577-z
Franceschini R, Rosi A, Catani F, Casagli N (2022b) Exploring a landslide inventory created by automated web data mining: the case of Italy. Landslides 19(4):841–853
Fukuhara M, Uchimura T, Wang L, Tao S, Tang J (2023) Study on the prediction of slope failure and early warning thresholds based on model tests. Geotechnics 4(1):1–17. https://doi.org/10.3390/geotechnics4010001
Giannecchini R, Galanti Y, D'Amato Avanzi G (2012) Critical rainfall thresholds for triggering shallow landslides in the Serchio River Valley (Tuscany, Italy). Nat Hazards Earth Syst Sci 12:829–842. https://doi.org/10.5194/nhess-12-829-2012
Gigli G, Lombardi L, Carla T, Beni T, Casagli N (2022) A method for full three-dimensional kinematic analysis of steep rock walls based on high-resolution point cloud data. Int J Rock Mech Min Sci 157:105178. https://doi.org/10.1016/j.ijrmms.2022.105178
Glade T, Crozier M, Smith P (2000) Applying probability determination to refine landslide-triggering rainfall thresholds using an empirical "antecedent daily rainfall model." Pure Appl Geophys 157:1059–1079. https://doi.org/10.1007/s000240050017
Guzzetti F (2000) Landslide fatalities and evaluation of landslide risk in Italy. Eng Geol 58:89–107. https://doi.org/10.1016/S0013-7952(00)00047-8
Guzzetti F, Gariano SL, Peruccacci S, Brunetti MT, Marchesini I, Rossi M, Melillo M (2020) Geographical landslide early warning systems. Earth-Sci Rev 200:102973. https://doi.org/10.1016/j.earscirev.2019.102973
Haque U, Blum P, Da Silva PF, Andersen P, Pilz J, Chalov SR, Keellings D (2016) Fatal landslides in Europe. Landslides 13:1545–1554. https://doi.org/10.1007/s10346-016-0689-3
Hastie T, Tibshirani R, Friedman J (2001) The elements of statistical learning. Springer-Verlag, New York. https://doi.org/10.1007/978-0-387-21606-5
Hofmann-Wellenhof B, Lichtenegger H, Collins J (2001) Applications of GPS. Global Positioning System: Theory and Practice. Springer Vienna, Vienna, pp 319–343
Huang X, Guo F, Deng M, Yi W, Huang H (2020) Understanding the deformation mechanism and threshold reservoir level of the floating weight-reducing landslide in the Three Gorges Reservoir Area, China. Landslides 17:2879–2894. https://doi.org/10.1007/s10346-020-01435-1
Huang G, Wang D, Du Y, Zhang Q, Bai Z, Wang C (2022) Deformation feature extraction for GNSS landslide monitoring series based on robust adaptive sliding-window algorithm. Front Earth Sci 10:884500. https://doi.org/10.3389/feart.2022.884500
Hungr O, Leroueil S, Picarelli L (2014) The varnes classification of landslide types, an update. Landslides 11:167–194. https://doi.org/10.1007/s10346-013-0436-y
Innocenti A, Pazzi V, Borselli L, Nocentini M, Lombardi L, Gigli G, Fanti R (2023) Reconstruction of the evolution phases of a landslide by using multi-layer back-analysis methods. Landslides 20(1):189–207. https://doi.org/10.1007/s10346-022-01971-y
Intrieri E, Gigli G, Mugnai F et al (2012) Design and implementation of a landslide early warning system. Eng Geol 147:124–136. https://doi.org/10.1016/j.enggeo.2012.07.017
Intrieri E, Gigli G, Casagli N, Nadim F (2013) Brief communication "landslide early warning system: toolbox and general concepts." Nat Hazard 13(1):85–90. https://doi.org/10.5194/nhess-13-85-2013
Jaboyedoff M, Carrea D, Derron MH, Oppikofer T, Penna IM, Rudaz B (2020) A review of methods used to estimate initial landslide failure surface depths and volumes. Eng Geol 267:105478. https://doi.org/10.1016/j.enggeo.2020.105478
Jordanova G, Gariano SL, Melillo M et al (2020) Determination of empirical rainfall thresholds for shallow landslides in Slovenia using an automatic tool. Water. https://doi.org/10.3390/w12051449
Kim SW, Chun KW, Kim M, Catani F, Choi B, Seo J (2021) Effect of antecedent rainfall conditions and their variations on shallow landslide

triggering rainfall thresholds in South Korea. Landslides 18(2):569–582. https://doi.org/10.1007/s10346-020-01505-4
Krøgli IK, Devoli G, Colleuille H, Boje S, Sund M, Engen IK (2018) The norwegian forecasting and warning service for rainfall-and snowmelt-induced landslides. Nat Hazards Earth Syst Sci 18(5):1427–1450. https://doi.org/10.5194/nhess-18-1427-2018
Mantovani F, Soeters R, Van Westen CJ (1996) Remote sensing techniques for landslide studies and hazard zonation in Europe. Geomorphology 15(3–4):213–225. https://doi.org/10.1016/0169-555X(95)00071-C
McColl ST, Cook SJ (2024) A universal size classification system for landslides. Landslides 21(1):111–120
Molnar C (2020). Interpretable machine learning. Available: https://christophm.github.io/interpretable-ml-book/
Mondini AC, Guzzetti F, Melillo M (2023) Deep learning forecast of rainfall-induced shallow landslides. Nat Commun 14(1):2466. https://doi.org/10.1038/s41467-023-38135-y
Nava L, Carraro E, Reyes-Carmona C, Puliero S, Bhuyan K, Rosi A, Monserrat O, Floris M, Meena SR, Galve JP, Catani F (2023) Landslide displacement forecasting using deep learning and monitoring data across selected sites. Landslides 20(10):2111–2129
Nocentini N, Rosi A, Segoni S, Fanti R (2023) Towards landslide space-time forecasting through machine learning: the influence of rainfall parameters and model setting. Front Earth Sci 11:1152130. https://doi.org/10.3389/feart.2023.1152130
Nocentini N, Medici C, Barbadori F, Gatto A, Franceschini R, del Soldato M, Segoni S (2024a) Optimization of rainfall thresholds for landslide early warning through false alarm reduction and a multi-source validation. Landslides 21(3):557–571. https://doi.org/10.1007/s10346-023-02176-7
Nocentini N, Rosi A, Piciullo L, Liu Z, Segoni S, Fanti R (2024b) Regional-scale spatiotemporal landslide probability assessment through machine learning and potential applications for operational warning systems: a case study in Kvam (Norway). Landslides 21(10):2369–2387. https://doi.org/10.1007/s10346-024-02287-9
Notti D, Cina A, Manzino A, Colombo A, Bendea IH, Mollo P, Giordan D (2020) Low-cost GNSS solution for continuous monitoring of slope instabilities applied to Madonna del Sasso Sanctuary (NW Italy). Sensors 20(1):289
Patton AI, Rathburn SL, Capps DM (2019) Landslide response to climate change in permafrost regions. Geomorphology 340:116–128. https://doi.org/10.1016/j.geomorph.2019.04.029
Peressi, G. (2019) Frana di Cazzaso. Relazione tra spostamenti e precipitazioni. Regione Autonoma Friuli Venezia giulia – Protezione Civile della Regione. 1–18.
Piciullo L, Calvello M, Cepeda JM (2018) Territorial early warning systems for rainfall-induced landslides. Earth-Sci Rev 179:228–247. https://doi.org/10.1016/j.earscirev.2018.02.013
Pratesi F, Nolesini T, Bianchini S, Leva D, Lombardi L, Fanti R, Casagli N (2015) Early warning GBInSAR-based method for monitoring Volterra (Tuscany, Italy) city walls. IEEE J Sel Top Appl Earth Obs Remote Sens 8(4):1753–1762. https://doi.org/10.1109/JSTARS.2015.2402290
Rahul S, Tyagi A (2025) Physics-based time-of-failure determination of rainfallinduced instability in lateritic soil slopes. Eng Geol 344:107834
Ramella R, Roberto R. Prosecuzione di un Incarico per il Monitoraggio del Dissesto Franoso Interessante L'abitato di Cazzaso in Comune di Tolmezzo (UD) Convenzione Rep. 7872 dd. 30 Dicembre 2002, Secondo Rapporto Annuale, REL/75–2004/RIMA-02; Technical Report Realised by OGS; OGS: New York, NY, USA, 2004.
Reichenbach P, Rossi M, Malamud BD, Mihir M, Guzzetti F (2018) A review of statistically-based landslide susceptibility models. Earth-Sci Rev 180:60–91
Rosi A, Lagomarsino D, Rossi G, Segoni S, Battistini A, Casagli N (2015) Updating EWS rainfall thresholds for the triggering of landslides. Nat Hazards 78:297–308. https://doi.org/10.1007/s11069-015-1717-7
Rosi A, Peternel T, Jemec-Auflič M, Komac M, Segoni S, Casagli N (2016) Rainfall thresholds for rainfall-induced landslides in Slovenia. Landslides 13:1571–1577. https://doi.org/10.1007/s10346-016-0733-3
Rosi A, Segoni S, Canavesi V, Monni A, Gallucci A, Casagli N (2021) Definition of 3D rainfall thresholds to increase operative landslide early warning system performances. Landslides 18:1045–1057. https://doi.org/10.1007/s10346-020-01523-2
Rosi A, Frodella W, Nocentini N, Caleca F, Havenith HB, Strom A, Tofani V (2023) Comprehensive landslide susceptibility map of Central Asia. Nat Hazards Earth Syst Sci 23(6):2229–2250
Rossi G, Zuliani D, Fabris P (2016) Long-term GNSS measurements from the northern Adria microplate reveal fault-induced fluid mobilization. Tectonophysics 690:142–159. https://doi.org/10.1016/j.tecto.2016.04.031
Rossi G, Fabris P, & Zuliani D (2018). Overpressure and fluid diffusion causing non-hydrological transient GNSS displacements. In Geodynamics and Earth Tides Observations from Global to Micro Scale (pp. 275–294). Cham: Springer International Publishing. https://doi.org/10.1007/978-3-319-96277-1_20
Salee R, Chinkulkijniwat A, Yubonchit S et al (2022) New threshold for landslide warning in the southern part of Thailand integrates cumulative rainfall with event rainfall depth-duration. Nat Hazards 113:125–141. https://doi.org/10.1007/s11069-022-05292-0
Sapena M, Gamperl M, Kühnl M, Garcia-Londoño C, Singer J, Taubenböck H (2023) Cost estimation for the monitoring instrumentalization of landslide early warning systems. Nat Hazards Earth Syst Sci Discuss 2023:1–26. https://doi.org/10.5194/nhess-23-3913-2023
Sättele M, Krautblatter M, Bründl M, Straub D (2016) Forecasting rock slope failure: how reliable and effective are warning systems? Landslides 13:737–750
Schlögl M, Spiekermann R, Steger S (2025) Towards a holistic assessment of landslide susceptibility models: insights from the Central Eastern Alps. Environ Earth Sci 84:113. https://doi.org/10.1007/s12665-024-12041-y
Segalini A, Valletta A, Carri A (2018) Landslide time-of-failure forecast and alert threshold assessment: a generalized criterion. Eng Geol 245:72–80. https://doi.org/10.1016/j.enggeo.2018.08.003
Šegina E, Peternel T, Urbančič T, Realini E, Zupan M, Jež J, Auflič MJ (2020) Monitoring surface displacement of a deep-seated landslide by a low-cost and near real-time GNSS system. Remote Sens 12(20):3375. https://doi.org/10.3390/rs12203375
Segoni S, Rosi A, Rossi G, Catani F, Casagli N (2014a) Analysing the relationship between rainfalls and landslides to define a mosaic of triggering thresholds for regional scale warning systems. Nat Hazards Earth Syst Sci 14:2637–2648. https://doi.org/10.5194/nhessd-2-2185-2014
Segoni S, Rossi G, Rosi A, Catani F (2014b) Landslides triggered by rainfall: a semi-automated procedure to define consistent intensity-duration thresholds. Comput Geosci 63:123–131. https://doi.org/10.1016/j.cageo.2013.10.009
Segoni S, Piciullo L, Gariano SL (2018a) A review of the recent literature on rainfall thresholds for landslide occurrence. Landslides 15(8):1483–1501
Segoni S, Rosi A, Lagomarsino D, Fanti R, Casagli N (2018b) Brief communication: using averaged soil moisture estimates to improve the performances of a regional-scale landslide early warning system. Nat Hazards Earth Syst Sci 18:807–812. https://doi.org/10.5194/nhess-18-807-2018
Solari L, Bianchini S, Franceschini R, Barra A, Monserrat O, Thuegaz P, Catani F (2020) Satellite interferometric data for landslide intensity evaluation in mountainous regions. Int J Appl Earth Obs Geoinf 87:102028. https://doi.org/10.1016/j.jag.2019.102028
Steger S, Moreno M, Crespi A, Luigi Gariano S, Teresa Brunetti M, Melillo M, Peruccacci S, Marra F, de Vugt L, Zieher T, Rutzinger M, Mair V, Pittore M (2024) Adopting the margin of stability for space–time landslide prediction – a data-driven approach for generating spatial dynamic thresholds. Geosci Front. https://doi.org/10.1016/j.gsf.2024.101822
Tehrani FS, Calvello M, Liu Z, Zhang L, Lacasse S (2022) Machine learning and landslide studies: recent advances and applications. Nat Hazards 114(2):1197–1245
Thiebes B, Glade T (2018) Landslide early warning systems—fundamental concepts and innovative applications. In Landslides and engineered slopes. Experience, theory and practice (pp. 1903–1911). CRC Press

Trigila A, Iadanza C, Guerrieri L, Hervás J (2007) The IFFI project (Italian landslide inventory): methodology and results. Guide Map Areas Risk Landslides Eur 23:15

Tunini L, Zuliani D, Di Traglia F, Borselli L, De Luca C, Nolesini T, Casu F (2024a) Monitoring and modelling moraine landslides: an example from Cazzaso village (Carnic Alps, Italy). Bullet Geophysics Oceanograp 65(3):327–346. https://doi.org/10.4430/bgo00459

Tunini L, Magrin A, Rossi G, Zuliani D (2024b) Global navigation satellite system (GNSS) time series and velocities about a slowly convergent margin processed on high-performance computing (HPC) clusters: products and robustness evaluation. Earth Syst Sci Data 16(2):1083–1106. https://doi.org/10.5194/essd-16-1083-2024

Vallet A, Varron D, Bertrand C, Fabbri O, Mudry J (2016) A multi-dimensional statistical rainfall threshold for deep landslides based on groundwater recharge and support vector machines. Nat Hazards 84(2):821–849. https://doi.org/10.1007/s11069-016-2453-3

Wicki A, Lehmann P, Hauck C, Seneviratne SI, Waldner P, Stähli M (2020) Assessing the potential of soil moisture measurements for regional landslide early warning. Landslides 17:1881–1896. https://doi.org/10.1007/s10346-020-01400-y

Wu S, Hu X, Zheng W, Berti M, Qiao Z, Shen W (2021) Threshold definition for monitoring Gapa landslide under large variations in reservoir level using GNSS. Remote Sens 13(24):4977. https://doi.org/10.3390/rs13244977

Zêzere JL, Vaz T, Pereira S, Oliveira SC, Marques R, Garcia RA (2015) Rainfall thresholds for landslide activity in Portugal: a state of the art. Environ Earth Sci 73:2917–2936. https://doi.org/10.1007/s12665-014-3672-0

Zhou CH, Lee CF, Li J, Xu ZW (2002) On the spatial relationship between landslides and causative factors on Lantau Island, Hong Kong. Geomorphology 43(3–4):197–207

Zuliani D, Tunini L, Di Traglia F, Chersich M, Curone D (2022a) Cost-effective, single-frequency GPS network as a tool for landslide monitoring. Sensors 22(9):3526. https://doi.org/10.3390/s22093526

Zuliani D, Tunini L, Severin M, Bertoni M, Ponton C, Parolai S (2022b) LZER0: a cost-effective multi-purpose GNSS platform. Sensors 22(21):8314. https://doi.org/10.3390/s22218314

Zuliani D, Fabris P, & Rossi G (2018). FReDNet: evolution of a permanent GNSS receiver system. In New Advanced GNSS and 3D Spatial Techniques: Applications to Civil and Environmental Engineering, Geophysics, Architecture, Archeology and Cultural Heritage (pp. 123–137). Springer International Publishing. https://doi.org/10.1007/978-3-319-56218-6_10

Rachele Franceschini (✉) · Lavinia Tunini · David Zuliani · Giuliana Rossi
National Institute of Oceanography and Applied Geophysics – OGS, Trieste, Italy
Email: rfranceschini@ogs.it

Nicola Nocentini
Department of Earth Sciences, University of Firenze, Via Giorgio La Pira, 4, 50121 Florence, Italy

Ascanio Rosi
Department of Geosciences, University of Padova, Via G. Gradenigo, 6, 35131 Padua, Italy

Gabriele Peressi
Department of Civil Protection of Friuli Venezia Giulia Region, Via Natisone 43, 33057 Palmanova, Udine, Italy